between the results of the CRDS and the turbidimetry. The results are shown in Figure 5. It should be noted that due to low precision, small sensitivity, no linearity as well as presence of high interference, turbidimetry cannot be adopted for detection of phosphorous species instead of CRDS. Consequently, turbidimetry as the detection system was only used to approve the scattering phenomenon.

Phosphorus species like any other salt had tendency to hydration. This phenomenon, therefore, changed the size and thickness of the hydrated layer [39]. This effect also converted the hygroscopic growth factor, and thus changing in the scattering and turbidity.

In the H_2/air flame, H_2O was considered as a product according to the flowing reactions (Eqs. 4 and 5). Based on these results, aerosols containing compounds such as phosphorus species provide the ability to absorb H_2O molecules from surrounding environment their size is larger [39]. The main reason for this was that the mass scattering efficiency of aerosols would increase when water soluble aerosols grow to become larger in diameter. Consequently, at low concentrations the scattering phenomenon was majorly occurred in comparison with luminescence radiation. This phenomenon can also be interpreted somewhat like the formation of crystal salts in a supper saturated solution. The lower concentration of salts, the larger crystalline size is generated; therefore, larger aerosols (i.e., more hydration no.) are expected from diluted phosphorous species.

$$H_2+O_2 \rightarrow 2OH \quad \text{(Eq. 4)}$$

$$H_2+OH^{\cdot} \rightarrow H^{\cdot}+H_2O \quad \text{(Eq. 5)}$$

A reverse correlation was observed between the relative humidity percentage (RH%) and concentrations of PO_4^{3-} at ng mL^{-1} levels in different environments such as about 15 and 45% RH according to the results shown in Figure 6. This behavior again pointed to the effective role of hygroscopic growth factor during scattering the phosphorous species inside H_2/air flame, which generated water as the product of the reaction between hydrogen and oxygen (Eqs. 4 and 5). This result was in good agreement with the results obtained during estimation of the scattering radiation using instruments such as online forward-scatter visibility meter, integrating nephelometer and multi-angle absorption photometer [39].

Hygroscopic growth factor was also defined as the ratio of aerosol scattering coefficient, $f_{(RH)}$ at wet condition to that at dry condition (RH ≤ 30%) according to the equation reported in Ref. [39]. In this system, based on the results shown in Figure 6, the RH% of the two different conditions (RH% 15 and 45) was found to be 1.36, which pointed to the effective role of the environmental RH%. This factor was considered as aerosol particle backscatter coefficient, which was dependent on the size and morphology of the aerosols particles [43]. The relationship between the hygroscopic growth effects and the aerosol volume concentration was evaluated by observing a stronger increase in the fine mode volume concentration of the phosphorous-containing aerosols during increase in the quantity of RH% inside the H_2/air flame.

The relationship between the size of aerosols and the phosphorous concentration can also be evaluated via following the hydration number of the phosphorous species. In this study, the same behavior can be observed for phosphorous species inside a humid flame generated using H_2 and O_2. However, hydration number of phosphorus aerosol can be discussed using the extended Debye-Hückel equation using the parameter called "mean distance approach of the hydrated ions". Based on this term, the thicker the hydrated layer of phosphorus species, the more was the activity coefficient and the higher was the activity of phosphorus species.

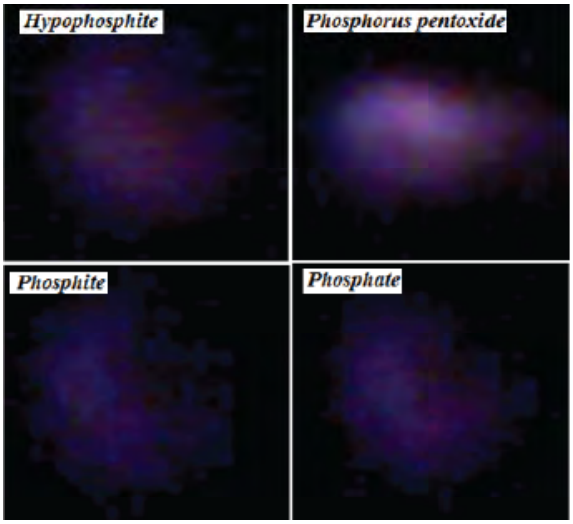

Figure 7: CCD images related to the introduction of various phosphorous species to the CRDS system.

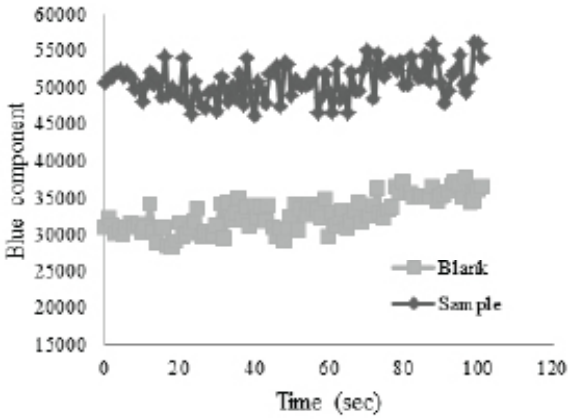

Figure 8: Trace diagram during analysis of PO_4^{3-} 10.0 µg mL^{-1}.

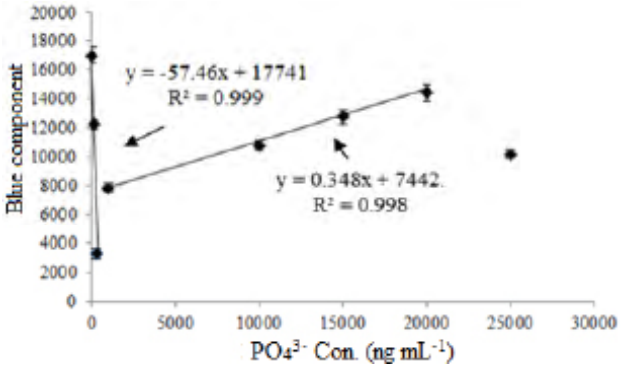

Figure 9: Calibration curve of phosphorous compounds at ng mL^{-1} and µg mL^{-1} levels.

The intensity of the scattered light was independent from that proposed by Saha equation [44]. The Saha ionization equation was an expression that relates the ionization state of an element to the temperature and pressure. In this study the Saha equation described the

Linear dynamic range	Correlation coefficient (R)	Calibration sensitivity	RSD (%)	Detection limit (ng mL^{-1})
PO_4^{3-} (1-20 µg mL^{-1})	0.998	0.348	11.0	-
PO_4^{3-} (10-250 ng mL^{-1})	0.999	-57.46	12.0	5

Table 1: Analytical figures of merit during phosphorus detection and determination. Note: The data are the average of 70 sequential analyses.

Foreign species	Tolerance ratio	Interfering effect (%)	Comments
CH_3COO^-, Cl^-, Br^-, ClO_4^-, I^-, CN^-, COO^-, CO_3^{2-}	1000	No interference	-No interaction with phosphorus species -Not emission radiation
NO_3^-	500	~3% enhancement	-No interaction with phosphorus species -Low emission radiation
K^+, Co^{2+}	500	No interference	-No interaction with phosphorus species -Not emission radiation
NH_4^+	1000	No interference	-No interaction with phosphorus species -Not emission radiation
Ca^{2+}	500	No interference	interaction with phosphorus species and formation precipitate Calcium phosphate (K_{SP}=2.07 × 10^{-33})
Fe^{3+}	500	No interference	interaction with phosphorus species and formation precipitate iron phosphate (K_{SP}=1.3 × 10^{-22})
Ni^{2+}	500	No interference	interaction with phosphorus species and formation precipitate nickel phosphate (K_{SP}=4.74 × 10^{-32})
SO_4^{2-}	200	~20% Enhancement	Molecular emission of sulfur

Table 2: Effect of foreign species on phosphorus determination.

Methods	Analyzed sample	Linear range	Detection limit	Reference
Spectrophotometry	Seawater	0.034-1.134 µM (3.213-107.163 ng mL^{-1})	1.4 nM (0.1323 ng mL^{-1})	[48]
Fluorimetry	River and marine waters	0.3-4.0 µM (28.35-378 ng mL^{-1})	0.3 µM (28.35 ng mL^{-1})	[49]
Spectrophotometry	Wastewater	0.026-0.485 mM (2475-45832 ng mL^{-1})	7.4 µM (699.3 ng mL^{-1})	[50]
Electrochemiluminescence	Water	2.0 × 10^{-10}-1.0 × 10^{-8} gmL^{-1} (0.2-10 ng mL^{-1})	8.0 × 10^{-11} gmL^{-1} (0.08 ng mL^{-1})	[36]
Electrochemistry	Human serum sample	1.0 × 10^{-6}- 100.0 × 10^{-6} mol L^{-1} (94.5-945000 ng mL^{-1})	3 × 10^{-6} mol L^{-1} (283.5 ng mL^{-1})	[51]
Ion exchange chromatography	Drug product	2-200 µg mL^{-1} (2000-200000 ng mL^{-1})	1 µg mL^{-1} (1000 ng mL^{-1})	[52]
Present study	Drinking water	10.0-250.0 ng mL^{-1} and 1.0-20.0 µg mL^{-1} or (1000-20000 ng mL^{-1})	5.0 ng mL^{-1}	This work

Real sample	Proposed method (ng mL^{-1})	[1]Ion exchange chromatography (ng mL^{-1})	Relative error (%)
Drinking water 1	19.00	19.51	-2.60
Drinking water 2	17.01	17.30	-1.68
Drinking water 3	10.15	10.43	-2.68
Well water1	25.82	26.35	-2.01
Well water 2	8.71	8.43	+3.32

Table 3: Real sample analysis. Where, [1]Ion exchange chromatography was considered as Ref. method [47].

Electrochemistry	Human serum sample	1.0 × 10^{-6}- 100.0 × 10^{-6} mol L^{-1} (94.5-945000 ng mL^{-1})	3 × 10^{-6} mol L^{-1} (283.5 ng mL^{-1})	[51]
Ion exchange chromatography	Drug product	2-200 µg mL^{-1} (2000-200000 ng mL^{-1})	1 µg mL^{-1} (1000 ng mL^{-1})	[52]
Present study	Drinking water	10.0-250.0 ng mL^{-1} and 1.0-20.0 µg mL^{-1} or (1000-20000 ng mL^{-1})	5.0 ng mL^{-1}	This work

Table 4: Comparison between the introduced method and the previously reported method.

degree of ionization of the atomizer as a function of the temperature, density, and ionization energies of the species [45]. If Saha ionization occurred, the amount of emission would increase a little. However the Saha equation only held weakly ionized plasmas for in which the Deby length was large [46,47]. The independency of the scattered light with the Saha phenomenon was evidenced via observation of no significant response during independently analysis of inorganic species such as Na^+, K^+ or H_3PO_4. Consequently, this phenomenon clearly pointed to the presence of strong interaction between Na^+ and phosphorous species during introduction of aerosols to the H_2/air flame.

Based on this principle, trace quantity of Na^+ ions as radiation buffer was stabilized inside the flame and played a role such as the incident laser light for scattering process, resulting to get blue radiation instead of green chemiluminescence of phosphorous species or even

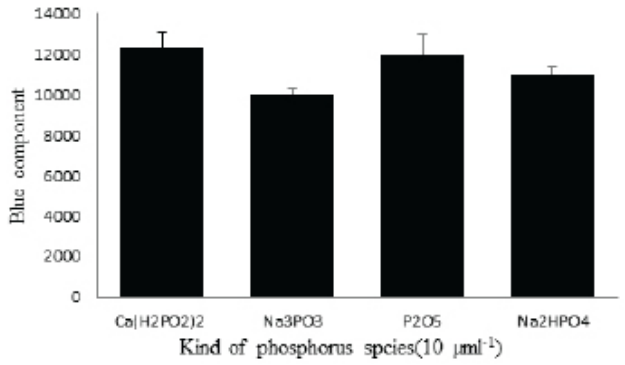

Figure 10: Effect of various kinds of phosphorus species 10 μg mL^{-1} at pH 2.6.

the emission of Na^+/Na inside the flame. All these evidences pointed to the effective role of a parameter called hygroscopic growth factor during formation of aerosols.

Analytical figures of merit

Figure 7 exhibits the CCD images related to the introduction of various phosphorous species to the CRDS system. Figure 8 shows sample trace diagram during analysis of po_4^{3-} (10.0 μg mL^{-1}) during the image analysis. The calibration curves had also been shown in Figure 9. As shown, the calibration curves had two significant linear ranges. Based on the calibration curve, sensitivity with positive slope was observed in the emission intensity depending on the concentration of phosphorus species at μg mL^{-1} levels during both scattering and luminescence phenomena. Whereas reverse behavior was exhibited during analysis of phosphorous compounds at ng mL^{-1} levels by the scattering phenomena. Based on the literature, this was related to the "Aerosol Hygroscopic Growth Factor" [39]. Two linear calibration curves with reverse slope was therefore observed between 10.0 – 250.0 ng mL^{-1} and 1.0 – 20.0 μg mL^{-1} with correlation coefficients (R^2) of 0.998 and 0.999, respectively (Figure 9). The calibration sensitivity was also estimated to be 0.348 and -57.46 (a.u.), respectively.

The detection limit was defined as the concentration of phosphorous species giving a signal equal to the blank signal plus triple values of the standard deviation of the blank. Based on this definition, the limit of detection was found as 5.0 ng mL^{-1}.

The relative standard deviation (RSD%, reproducibility) for 5 replicate analyses for each 10.0 ng mL^{-1} and 10.0 μg mL^{-1} PO_4^{3-} was found to be 12.0 and 11.0%, respectively. Based on the definition of the response time, 90% of maximum response (t_{90}), the maximum response time was evaluated to be ~10.0 s. Table 1 shows analytical figures of merit during phosphorus detection and determination.

Figure 10 compares the HPO* emissions measured during the introduction of 3.0 mL of each phosphorus in 10.0 μg mL^{-1} solution to the reaction cell containing 20.0 mL $HClO_4$ at pH 2.6. As shown partially the same emission intensity was detected during introduction of 10.0 μg mL^{-1} of each phosphorous species such as Na_2HPO_4 (RSD=4.3%, n=28), Na_3PO_3 (RSD%=6.1%, n=37), $Ca(H_2PO_2)_2$ (RSD=6.1%, n=38), and P_2O_5 (RSD=6.8%, n=40) at pH ~2.6.

No serious interference was evaluated during analysis of at least 500-fold excess of various anions such as CH_3COO^-, Cl^-, Br^-, ClO_4^-, I^-, CN^-, CO_3^{2-}, NO_3^-, I_3^- and various cations such as, NH_4^+, Na^+, Fe^{3+}, K^+, Ni^{2+}, CO^{2+}, Ca^{2+} to a 10.0 μg mL^{-1} and 10.0 ng mL^{-1} of phosphate standard solution. The results are reported in Table 2. The only observed interference was evaluated during introduction of 200-fold excess of SO_4^{2-}. These results clearly pointed to the selectivity of the recommended technique for rapid and sensitive determination of phosphorous species in various real samples without any interfering effects.

Real sample analyses

The reliability of this method was evaluated via selective determination of phosphorus in various drinking water samples according to the recommended preparation procedure. For this purpose standard addition method was used during the analyses of some drinking water samples. The results are reported in Table 3. As shown good correlation was evaluated between the results obtained from this technique and ion exchange chromatography during analysis of drinking water samples that clearly revealed the reliability of this method for detection and determination of species such as phosphorus compounds.

Conclusions

In this study, a new method has been introduced based on aerosol hygroscopic growth as a new factor for trace and ultra-trace determination of phosphorus in flame containing OT-CRDS. The advantages and disadvantages of the technique for phosphorous determination have been compared to the articles shown in Table 4. Compared to these reports, this technique has significant characteristics such as high sensitivity, high selectivity, capability to determine phosphorus compounds in a wide range between 10.0 - 250.0 ng mL^{-1} and 1.0 to 20.0 μg mL^{-1} with improved detection limit, simplicity, and low cost. To the best of our knowledge this study is the first report that Mie scattering is followed for determination purposes using a simple design of OT-CRDS.

Acknowledgements

The authors wish to acknowledge the support of this work by the Shiraz University Research Council.

References

1. Bao XP, Zhou YH, Yu JH (2010) N-Salicyloyltryptamine: An efficient fluorescent turn-on chemosensor for F− and AcO− based on an increase in the rigidity of the receptor. Luminescence 130: 392-398.
2. Kaur N, Kaur S, Kaur A, Saluja P, Sharma H, et al. (2014) Nanoparticle-based, organic receptor coupled fluorescent chemosensors for the determination of phosphate. Luminescence 145: 175-179.
3. Worsfold PJ, Gimbert LJ, Mankasingh U, Omaka ON, Hanrahan G, et al. (2005) Sampling, sample treatment and quality assurance issues for the determination of phosphorus species in natural waters and soils. Talanta 66: 273-293.
4. Mulkerrins D, Dobson A, Colleran E (2004) Parameters affecting biological phosphate removal from wastewaters. Environment International 30: 249-259.
5. Berchmans S, Issa TB, Singh P (2012) Determination of inorganic phosphate by electroanalytical methods: A review. Anal Chim Acta 729: 7-20.
6. Kawasaki H, Sato K, Hasegawa JOY, Yuki H (1989) Determination of inorganic phosphate by flow injection method with immobilized enzymes and chemiluminescence detection. Anal Biochem 812: 366-370.
7. Kwan RCH, Leung HF, Hon PYT, Cheung HCF, Hirota K, et al. (2005) Amperometric biosensor for determining human salivary phosphate. Anal Biochem 343: 263-267.
8. Larsen MJ, Jensen AF, Madsen DM, Pearce EI (1999) Individual variations of pH, buffer capacity, and concentrations of calcium and phosphate in unstimulated whole saliva. Archiv Oral Biolog 44: 111-117.
9. Tobey SL, Anslyn EV (2003) Determination of inorganic phosphate in serum and saliva using a synthetic receptor. Organic Lett 5: 2029-2031.